

Multiobjective Optimization for PI-based Control Strategies for HVAC Systems in Coaches

María Luisa Delgado*, Mario L. Ruz**, Francisco Vázquez*, Jorge E. Jiménez-Hornero*

* *Department of Electrical Engineering and Automatic Control, University of Cordoba, Campus Rabanales, 14071 Cordoba, Spain (e-mail: p72degum@uco.es, fvazquez@uco.es, jjimenez@uco.es).*

** *Department of Mechanics, University of Cordoba, Campus Rabanales, 14071 Cordoba, Spain (e-mail: mario.ruz@uco.es)*

Abstract: Thermal comfort in vehicles is crucial for several reasons, including safety, health and well-being of the passengers, energy efficiency and customer satisfaction. Heating, Ventilation and Air Conditioning (HVAC) systems and their control play an important role in achieving comfortable thermal conditions, so one of the most important steps to carry out is a correct tuning of the control loop parameters. In this work, two heating control strategies, specifically designed for coaches, are presented. The proposed schemes are based on PI controllers whose parameters are tuned using Multiobjective Optimization (MOO), where several cost functions related to cabin comfort and energy consumption (crucial in electric coaches) are used. For the tuning task, firstly, a multidimensional Pareto front approximation is obtained based on a set of metrics, such as the Integral Square Error (ISE) and the Total Variation (TV), among others. The set of optimal solutions is collected, and secondly, a Multiple Criteria Decision Making (MCDM) method is used to select an optimal solution from the Pareto set, specifically, the Technique for Order of Preference by Similarity to Ideal Solution (TOPSIS) method. The control schemes are compared by simulation using the Matlab/Simulink software. The results show good performance of both control strategies in reference tracking and the usefulness of the MOO approach in the tuning procedure.

Keywords: Parametric control optimization; control system design; genetic algorithms; simulation; control of systems in vehicles.

1. INTRODUCTION

The design, optimization, and control of Heating, Ventilation and Air Conditioning (HVAC) systems are essential to maintain human thermal comfort (Ruz et al., 2017). HVAC systems installed in public transport vehicles must operate over a wide range of operating conditions influenced by several external factors, such as solar irradiance or outdoor temperatures. In addition, coaches have inherent characteristics that differentiate them from other vehicles and make it difficult to control their HVAC systems, such as low insulation to reduce the weight of the body, variable passenger occupancy (He et al., 2018), disturbances caused by the opening/closing of their doors (Pathak et al., 2020) or the non-linear behavior of its internal components (Vázquez et al., 2023).

For heating the cabin in combustion vehicles, the used energy source comes from the engine cooling system. Currently, some restrictions make it difficult to control these systems when they work in heating mode, due to the Euro VI and later regulations against emissions recently applied, which limit the heat input provided by the combustion engine before reaching its optimum temperature (Delgado et al., 2023). In addition to the difficulties in heating control, in electric vehicles the battery is the source of energy for the heating system, which can lead to a reduction of up to 50% of its autonomy in winter (Schaut and Sawodny, 2020), (Ramsey et al., 2022), so the energy

consumed by the HVAC system should be reduced as far as possible, maintaining suitable comfort conditions in the cabin.

Due to its simplicity, one of the most popular methods for controlling vehicle HVAC systems is the rule-based on-off control scheme (Xie et al., 2020). More advanced techniques are proposed in the literature, e.g., adaptive and intelligent control algorithms such as neural networks, fuzzy control (Rajeswari Subramaniam et al., 2023), or Model Predictive Controller (MPC) (Xie et al., 2021). Nevertheless, control strategies based on PID controllers (Skogestad, 2023) are still widely used for HVAC system control due to their high efficiency, robustness and ease of implementation. Within the methodologies of PI tuning, it is common to set up the controller parameters employing tuning rules based on a simple model of the process dynamics, e.g., First Order Plus Time Delay (FOPTD) (Ruz et al., 2018). In addition, the increasing computing power has allowed the use of optimization algorithms to formulate the tuning task as an optimization problem with several conflicting design objectives to be optimized simultaneously (Neath et al., 2014), (Moya et al., 2017). The set of optimal solutions when no objective can be improved is called the Pareto Front, and a specific solution must be chosen. Multi Criteria Decision Making (MCDM) methods can be used to select one of the optimal solutions from the Pareto front (Opricovic and Tzeng, 2004).

This work is primarily focused on the design of PI-based control strategies for HVAC coaches, where two control schemes are proposed and tuned by means of Multiobjective Optimization (MOO). The problem considers five objective functions: two related to the error (difference between set point and real temperature) in the driver's zone temperature, two related to the smoothness of control actions, and one related to energy consumption. The obtained solutions are evaluated using a MCDM method, the Technique for Order of Preference by Similarity to Ideal Solution (TOPSIS) method.

The rest of the paper is organized as follows: Section 2 describes the coach thermal model, the two proposed control schemes and the tuning procedure for the control parameters. In section 3, the results obtained from the MOO problem are shown and the two control schemes are compared. Finally, Section 4 summarizes the conclusions.

2. METHODOLOGY

2.1 Coach thermal model

The main purpose of the developed model is to assess several heating control strategies with the final objective of enhancing thermal comfort and improving system performance. The model is based on previous works from the authors (Delgado et al., 2022), (Delgado et al., 2023). This model mainly consists of the following subsystems (Fig. 1): the coach cabin (driver's and passengers' zones), the driver's and the passengers' HVAC units, and the control system.

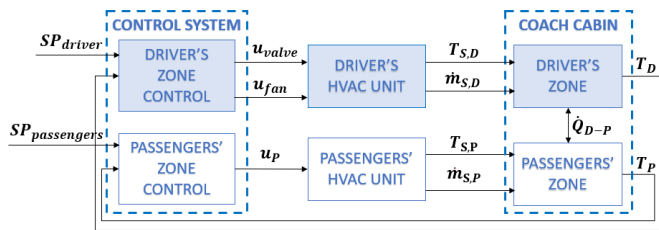


Figure 1. Block diagram of the controlled system.

The coach cabin thermal model is a lumped-parameter model based on energy balance equations that take into account the volume of interior air, the characteristics of the vehicle's windows, the number of people on board, the outside temperature and the incident solar radiation. Since there are two independent HVAC units, this model considers two thermal zones (driver's zone and passengers' zone) and the bidirectional heat exchange between them (\dot{Q}_{D-P}). The inputs

are the supply air temperatures for both zones ($T_{S,D}$ and $T_{S,P}$, respectively), the supply mass airflow rates ($\dot{m}_{S,P}$ and $\dot{m}_{S,D}$), and the outside air temperature (not shown in the figure). As model outputs, the mean interior temperatures of both zones (T_D and T_P) are considered. This work mainly focused on the driver's zone.

The driver's HVAC unit primarily consists of a compact cross-flow air-water heat exchanger, a water flow control valve, and a fan. In the heat exchanger, heat transfer occurs between the hot water from the engine cooling circuit and the air, which can be either recirculated from inside the coach or drawn from the external environment. The fan facilitates this heat exchange by sending air to the heat exchanger's coil through which the hot water flows. The water flow is controlled by a motorized valve responsible for regulating the flow of hot water circulating through the heat exchanger coil. The inputs of the driver's HVAC unit model are the engine temperature, the outside air temperature, the water flow control valve opening setpoint, the fan speed setpoint, and a door positioner to select the airflow: through the driver's front windows, through the driver's feet or a combination of both outputs. The main outputs of this model are the supply air temperature, the mass airflow rate and the temperature and flow rate of the water at the unit outlet. Fig. 2 shows the coach thermal model developed in Matlab/Simulink software.

In (Delgado et al., 2022), (Delgado et al., 2023) a preliminary version of the model was tested and validated with real data, obtained in coaches under different real conditions.

2.2 Control schemes

Cascade control is a simple, yet useful method commonly used for cabin temperature control in coaches. Typically, the desired temperature inside the driver's zone serves as the reference for the outer controller and the required air temperature at the HVAC system outlet is the reference for the inner controller, being its manipulated variable the opening of the water flow control valve. However, the driver's HVAC unit is a "multi-input single-output" (MISO) process with two independent variables that can be manipulated (valve opening and fan speed, the latter usually operating in open loop) and one process output (the supply air temperature). In this work, an extra control loop is added to the control scheme, using the fan speed as an additional manipulated variable in order to achieve suitable human comfort with the minimum energy cost.

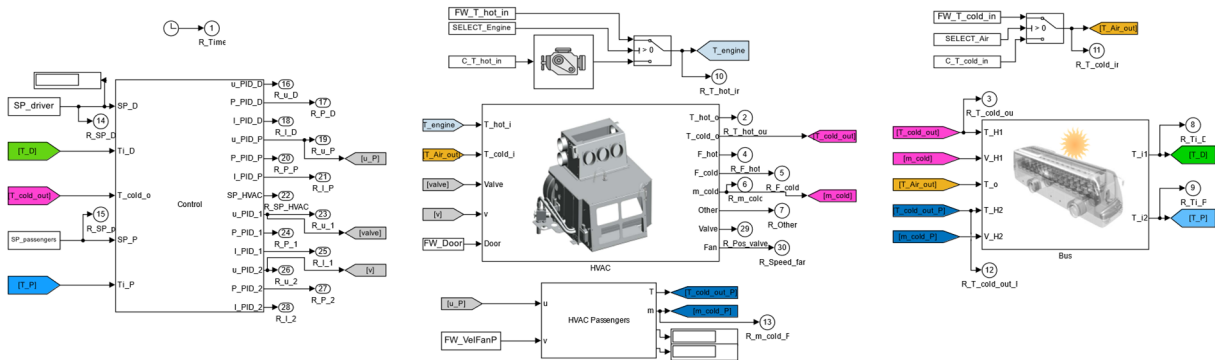


Figure 2. Coach thermal model.

Two PID-based control strategies are proposed, shown in Fig. 3 and Fig. 4. Each control scheme is composed of three PI controllers for the driver's zone. These blocks are implemented using Matlab code and include hysteresis and an anti-windup mechanism. In the control scheme *a* (Fig. 3), a cascaded control structure is used for the driver's zone. The PI controller of the outer loop (1 in the figure) has the temperature inside the driver's zone as controlled variable, while the inner loop is composed of two PI controllers (2 and 3) that have the supply air temperature from the HVAC unit of the driver's zone as controlled variable. The opening percentage of the water flow control valve and the percentage of fan speed, respectively are the manipulated variables. In contrast, in control scheme *b* (Fig. 4), the PI controller 3 is not in the inner loop and its controlled variable is the temperature inside the driver's zone. In both schemes, a programmed gain block is used to improve temperature control during vehicle start-up, very important in real coaches due to increasing engine temperature.

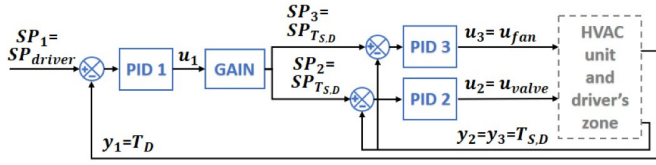


Figure 3. Control scheme *a*.

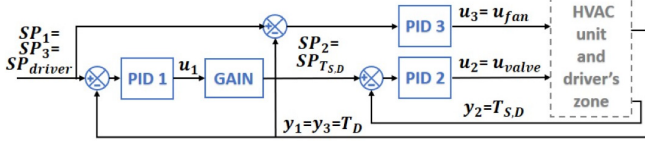


Figure 4. Control scheme *b*.

2.3 Tuning procedure

The PI controllers of the driver's zone are tuned for each proposed control scheme. For this purpose, a MOO problem was stated and solved using genetic algorithms. Equation (1) shows the vector of the design variables x composed of the proportional gain (K_P) and integral gain (T_I) of the PI controllers. The set of cost functions J is shown in (2).

$$x = [K_{P1} T_{I1} K_{P2} T_{I2} K_{P3} T_{I3}]^T \quad (1)$$

$$J = [ISE_{n1} TV_{u2} TV_{u3} MEC t_{Bn1}]^T \quad (2)$$

The normalized Integral Square Error (ISE_{n1}) between the PI controller 1 reference and the temperature inside the driver's zone is calculated using (3), where $e(k) = r_1(k) - y_1(k)$, N the number of samples, and T_s the sample time.

$$ISE_{n1} = \frac{1}{N} \sum_{k=1}^N \frac{e^2(k) + e^2(k-1)}{2} T_s \quad (3)$$

The total variation of the water flow control valve (TV_{u2}) is included as an objective function to extend the life of the water flow control valve. In addition, the total variation of the fan (TV_{u3}) is included to improve driver comfort, since changes in

the supply air flow rate can cause discomfort. These total variations are calculated as $TV_u = \sum_{k=1}^N |u(k) - u(k-1)|$.

The power consumed by the fan of the driver's HVAC unit is approximately proportional to its speed. The mean value of the manipulated variable of PI controller 3, corresponding to the fan speed, is proposed as another objective function. This mean energy consumption (MEC) is calculated by using (4).

$$MEC = \frac{1}{N} \sum_{k=1}^N u_3(k) \quad (4)$$

And finally, the time taken for the measured signal from PI controller 1 to enter and remain within the hysteresis band of the controller is considered as the last objective function, as shown in Fig. 5. This index, named t_{Bn1} , has been normalized by dividing by the total time.

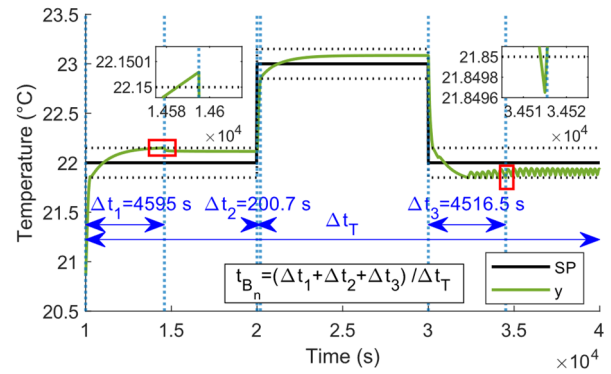


Figure 5. Hysteresis band index, t_{Bn1} . Note that for each change of reference, there is only one time interval.

The Matlab function *gamultiobj* (included in Global Optimization Toolbox) was used to solve the optimization problem; its main parameters have been configured as follows: a population size of 200, a maximum number of generations of 100, a Pareto front population fraction of 0.35, a crossover fraction of 0.8, and a function tolerance of 10^{-4} . In addition, for the design variables K_{P1} , K_{P2} and K_{P3} , the upper and lower bounds are set at 1 and 10^{-4} , respectively. The search range for T_{I1} , T_{I2} and T_{I3} is limited from 0.1 to 2000.

Once the multiple optimal solutions that compose the Pareto front are obtained, MCDM methods are used to select one of the front solutions. In this work, 70 solutions in the Pareto front are obtained and the TOPSIS method is used to select one of them. TOPSIS fundamental concept is that the selected solution should be the closest to the ideal solution and the farthest from the negative-ideal solution. For this purpose, the normalized decision matrix is first calculated, second the ideal and non-ideal solutions are determined for each criterion, and third, the Euclidean distance for each solution is calculated with respect to the ideal and non-ideal solutions. Finally, the solutions are ranked according to their relative proximity to the ideal solution.

3. EVALUATION

3.1 Pareto front

For each proposed control scheme, the MOO problem discussed in the previous section is addressed. For this purpose, a simulation of 40000 s is carried out, with changes in the PI 1 controller temperature reference (r_1). The first 10000 s are discarded in order to exclude motor start-up. The sample time of the PI controllers is 15 s, and the hysteresis and maximum and minimum values of the manipulated variables (u_{max} and u_{min} , respectively) are specified in Table 1. As an example, a cold day has been assumed, where the sun primarily shining on the rear part of the coach. The main parameters in the coach thermal model and their values are outside temperature (5 °C), frontal solar irradiance (30 W/m²), lateral solar irradiance (48 W/m²), back solar irradiance (445 W/m²), and mean temperature of the passengers' zone (21 °C approximately). The trapdoor to select the airflow in the driver's HVAC unit remains in a constant position, at 30 %.

The points obtained from the Pareto front of the two proposed control schemes for three of the objective functions are shown in Fig. 6, where the TV_{u2} and TV_{u3} indices are shown against the MEC index. The optimal solutions selected by the TOPSIS method are highlighted with a star (dark blue color for control scheme *a* and orange color for scheme *b*), where the solution for scheme control *a* obtains lower values for the aforementioned three indices.

Table 1. Fixed parameters of PI controllers

PI controller	u_{min}	u_{max}	Hysteresis band (°C)
1	0	1.5	± 0.15
2	0	1	± 0.3
3 <i>a</i>	0.15	1	± 0.3
3 <i>b</i>	0.15	1	± 0.15

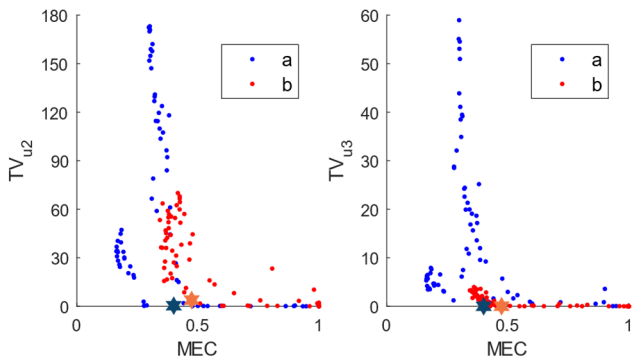


Figure 6. 2D projections of the Pareto fronts.

Table 2 shows the values of the cost functions and PI controller parameters for the optimal solution obtained using the TOPSIS method.

Table 2. Values of the cost functions and optimal parameters

Control scheme	ISE_{n1}	TV_{u2}	TV_{u3}	MEC	$t_{B_{n1}}$	K_{P1}	T_{i1}	K_{P2}	T_{i2}	K_{P3}	T_{i3}
<i>a</i>	0.0019	3.7208	0.0305	0.4002	0.1316	0.0691	373.38	0.1298	1095.61	0.0009	677.16
<i>b</i>	0.0012	38.3916	0.1727	0.4742	0.0132	0.1258	1011.15	0.4833	1006.61	0.6606	865.80

To compare the two proposed control strategies, once the Pareto front is obtained for each control scheme, the degradation level of each objective function is determined using the minimum and maximum values considering both Pareto fronts. By way of example, the level of degradation of the first considered objective function is calculated using (5). A degradation level equal to 0 indicates that the minimum value of the considered cost function has been chosen, while a value of 100 indicates that the algorithm has selected its maximum value as a solution within the Pareto fronts.

$$\alpha_{ISE_{n1}} = \frac{ISE_{n1} - \min (ISE_{n1})}{\max (ISE_{n1}) - \min (ISE_{n1})} \cdot 100 \quad (5)$$

A spider diagram showing the level of degradation of the cost functions for the optimal solution applying TOPSIS for each control scheme is shown in Fig. 7. In both control strategies, a very low degradation level percentage is obtained for the ISE_{n1} and TV_{u3} indexes. Strategy *a* has an improvement of 2% for TV_{u2} and more than 8% for MEC compared to *b*. However, the degradation value of the $t_{B_{n1}}$ index is higher in *a*.

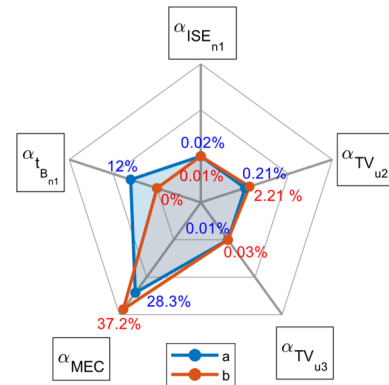


Figure 7. Spider diagram with the level of degradation of the cost functions.

3.2 Simulation results

The simulation results of the thermal model using the two proposed control schemes and the controller parameters from Table 2 are shown in Fig. 8 and Fig. 9, which show the results after start-up, once steady state has been reached. In this simulation, three setpoint changes are made to the driver's zone temperature. The first graph in Fig. 8 shows the setpoint (green line), the hysteresis band represented by dotted lines and the driver's zone temperature using each control scheme. The supplied air temperature from the HVAC unit of the driver's zone is shown in the second graph, as well as its setpoint. Finally, in Fig. 9, the manipulated variables of the PI controllers 2 and 3 are shown, i.e., those related to the valve opening and the fan speed (per unit).

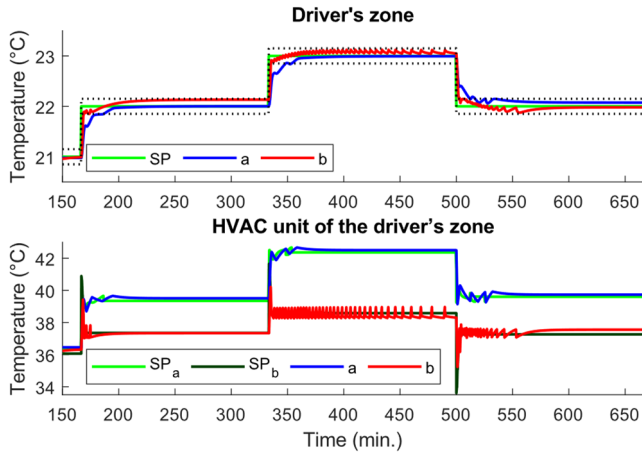


Figure 8. Simulation results for temperatures.

As observed in the simulation, reference tracking is good for both schemes. Strategy *b* is faster but, on the contrary, greater control variations are produced in the valve opening as well as higher energy consumption, as can be seen in the fan speed, which is higher during the entire simulation. To sum up, the plots shown are coherent with the index values specified in Table 2, also considering that the high variation of the valve opening in strategy *b* can pose a problem for practical implementations and, on the other hand, the largest energy consumption due to fan speed would be undesirable to be used in battery electric coaches. Therefore, scheme *a* should be chosen as the best option to obtain a better compromise solution.

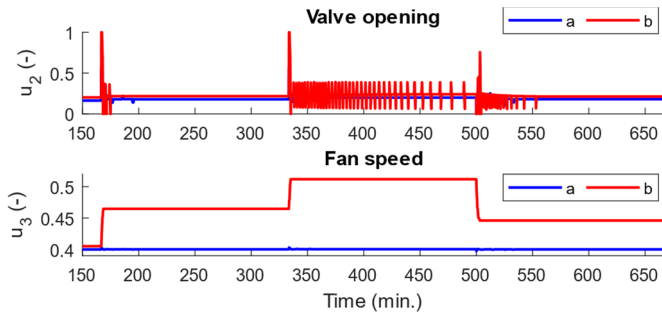


Figure 9. Simulation results for manipulated variables.

To test the robustness of scheme *a*, the system has been evaluated by changing the conditions (i.e. changing some of the parameter values with respect to the baseline case). Fig. 10 shows three examples. “1” represents a night journey with zero solar irradiance and outside temperature of 0 °C. In “2” the front and lateral solar irradiance are 200 W/m², and the back solar irradiance is 90 W/m². Finally, in “3” the mean temperature of the passengers’ zone is 23 °C.

Fig. 10 shows that the system accurately tracks the temperature reference in all three examples, imposing different setpoints for the air supply temperature in the inner control loop. The values obtained for the five performance indices used are shown in Table 3. These values are very similar to those obtained with the conditions imposed in the MOO problem. The main difference is found in example 2, with a greater variation in the valve opening.

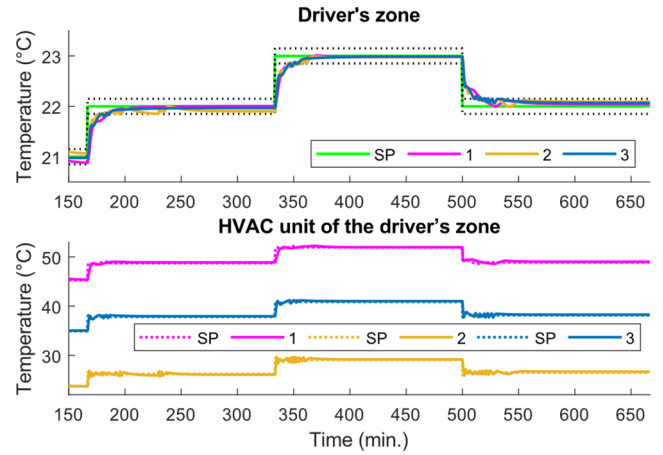


Figure 10. Simulation results under different conditions.

Table 3. Cost function values under different conditions

Example	ISE_{n1}	TV_{u2}	TV_{u3}	MEC	$t_{B_{n1}}$
1	0.0022	3.0519	0.0234	0.4006	0.1102
2	0.0019	9.5749	0.0742	0.4001	0.2220
3	0.0019	5.4190	0.0431	0.4002	0.1337

4. CONCLUSIONS

In this work, two control schemes for coach HVAC systems based on PI controllers have been proposed. The tuning task of these controllers has been addressed by using MOO, where genetic algorithms have been employed to obtain the optimal solutions from the Pareto front. Five objectives have been considered, one of them related to energy consumption (a key aspect for electric vehicles) and the remaining related to signal control variations and reference tracking performance. To select an optimal solution for each scheme, the TOPSIS method is used. Once the solution is selected, the two schemes have been compared, concluding that control scheme *a* produces better results with fewer changes in the valve opening and lower energy consumption, but it takes more time to reach the hysteresis band than scheme *b*. In addition, it is interesting to note that, for scheme *a*, the optimization procedure results in a specific constant fan speed value, which is equivalent to an open loop configuration, i.e., a constant air flow rate. In comparison to scheme *b*, despite having a slower dynamic response, strategy *a* results in lower energy consumption and less variation in control signals. Therefore, in simulation, it appears to be the more promising option.

In future research, the proposed strategies will be tested in a Hardware-in-the-loop (HIL) bench for coach HVAC systems at different operating points.

ACKNOWLEDGEMENTS

This work was supported by the Regional Government of Andalusia (Spain), under grant number P18-TP-2040, and by the Spanish Ministry of Science and Innovation (MCIN/AEI/10.13039/501100011033) and the European Union «NextGenerationEU/PRTR», under grant TED2021-130373B-I00.

REFERENCES

- Delgado, M.L., Jiménez-Hornero, J.E., Vázquez, F., 2023. Design, Implementation and Validation of a Hardware-in-the-Loop Test Bench for Heating Systems in Conventional Coaches. *Appl. Sci.* 13, 2212. <https://doi.org/10.3390/app13042212>
- Delgado, M.L., Jiménez, J., Vázquez, F., 2022. Modelo térmico de un sistema de calefacción para vehículos de transporte público, in: XLIII Jornadas de Automática: Libro de Actas: 7, 8 y 9 de Septiembre de 2022, Logroño (La Rioja). Servizo de Publicacións da UDC, pp. 500–507. <https://doi.org/10.17979/spudc.9788497498418.0500>
- He, H., Yan, M., Sun, C., Peng, J., Li, M., Jia, H., 2018. Predictive air-conditioner control for electric buses with passenger amount variation forecast☆. *Appl. Energy* 227, 249–261. <https://doi.org/10.1016/j.apenergy.2017.08.181>
- Moya, F., Rojas, J.D., Arrieta, O., 2017. Pareto-based polynomial tuning rule for 2DoF PID controllers for time-delayed dominant processes with robustness consideration. *Proc. Am. Control Conf.* 5282–5287. <https://doi.org/10.23919/ACC.2017.7963775>
- Neath, M.J., Swain, A.K., Madawala, U.K., Thrimawithana, D.J., 2014. An optimal PID controller for a bidirectional inductive power transfer system using multiobjective genetic algorithm. *IEEE Trans. Power Electron.* 29, 1523–1531. <https://doi.org/10.1109/TPEL.2013.2262953>
- Opricovic, S., Tzeng, G.H., 2004. Compromise solution by MCDM methods: A comparative analysis of VIKOR and TOPSIS. *Eur. J. Oper. Res.* 156, 445–455. [https://doi.org/10.1016/S0377-2217\(03\)00020-1](https://doi.org/10.1016/S0377-2217(03)00020-1)
- Pathak, A., Binder, M., Chang, F., Ongel, A., Lienkamp, M., 2020. Analysis of the Influence of Air Curtain on Reducing the Heat Infiltration and Costs in Urban Electric Buses. *Int. J. Automot. Technol.* 21, 147–157. <https://doi.org/10.1007/s12239-020-0015-x>
- Rajeswari Subramaniam, K., Cheng, C.T., Pang, T.Y., 2023. Fuzzy Logic Controlled Simulation in Regulating Thermal Comfort and Indoor Air Quality Using a Vehicle Heating, Ventilation, and Air-Conditioning System. *Sensors* 23. <https://doi.org/10.3390/s23031395>
- Ramsey, D., Bouscayrol, A., Boulon, L., Desreveaux, A., Vaudrey, A., 2022. Flexible Simulation of an Electric Vehicle to Estimate the Impact of Thermal Comfort on the Energy Consumption. *IEEE Trans. Transp. Electrif.* 8, 2288–2298. <https://doi.org/10.1109/TTE.2022.3144526>
- Ruz, M.L., Garrido, J., Vazquez, F., Morilla, F., 2018. Interactive tuning tool of proportional-integral controllers for first order plus time delay processes. *Symmetry (Basel)*. 10, 1–22. <https://doi.org/10.3390/sym10110569>
- Ruz, M.L., Garrido, J., Vázquez, F., Morilla, F., 2017. A hybrid modeling approach for steady-state optimal operation of vapor compression refrigeration cycles. *Appl. Therm. Eng.* 120, 74–87. <https://doi.org/10.1016/j.applthermaleng.2017.03.103>
- Schaut, S., Sawodny, O., 2020. Thermal Management for the Cabin of a Battery Electric Vehicle Considering Passengers' Comfort. *IEEE Trans. Control Syst. Technol.* 28, 1476–1492. <https://doi.org/10.1109/TCST.2019.2914888>
- Skogestad, S., 2023. Advanced control using decomposition and simple elements. *Annu. Rev. Control* 56, 100903. <https://doi.org/10.1016/j.arcontrol.2023.100903>
- Vázquez, F., Garrido, J., Ruz, M., Jiménez, J., 2023. Stiction compensation for low-cost electric valves. *Control Eng. Pract.* 134, 105482. <https://doi.org/10.1016/j.conengprac.2023.105482>
- Xie, Y., Liu, Z., Li, K., Liu, J., Zhang, Y., Dan, D., Wu, C., Wang, P., Wang, X., 2021. An improved intelligent model predictive controller for cooling system of electric vehicle. *Appl. Therm. Eng.* 182, 116084. <https://doi.org/10.1016/j.applthermaleng.2020.116084>
- Xie, Y., Liu, Z., Liu, J., Li, K., Zhang, Y., Wu, C., Wang, P., Wang, X., 2020. A Self-learning intelligent passenger vehicle comfort cooling system control strategy. *Appl. Therm. Eng.* 166. <https://doi.org/10.1016/j.applthermaleng.2019.114646>